AMERICAN SOCIETY FOR MICROBIOLOGY | mBio®

RESEARCH ARTICLE
Applied and Environmental Science

Members of the Genus *Methylobacter* Are Inferred To Account for the Majority of Aerobic Methane Oxidation in Oxic Soils from a Freshwater Wetland

Garrett J. Smith,[a] Jordan C. Angle,[a] Lindsey M. Solden,[a] Mikayla A. Borton,[a,b,c] Timothy H. Morin,[d] Rebecca A. Daly,[a,b] Michael D. Johnston,[e] Kay C. Stefanik,[a,f] Richard Wolfe,[a,b] Bohrer Gil,[c,f] Kelly C. Wrighton[a,b,c]

[a]Department of Microbiology, The Ohio State University, Columbus, Ohio, USA
[b]Department of Soil and Crop Sciences, Colorado State University, Fort Collins, Colorado, USA
[c]Environmental Science Graduate Program, The Ohio State University, Columbus, Ohio, USA
[d]Department of Environmental Resources Engineering, State University of New York College of Environmental Science and Forestry, Syracuse, New York, USA
[e]National Institute of Environmental Health Sciences, Durham, North Carolina, USA
[f]Department of Civil and Environmental Engineering and Geodetic Sciences, The Ohio State University, Columbus, Ohio, USA

ABSTRACT Microbial carbon degradation and methanogenesis in wetland soils generate a large proportion of atmospheric methane, a highly potent greenhouse gas. Despite their potential to mitigate greenhouse gas emissions, knowledge about methane-consuming methanotrophs is often limited to lower-resolution single-gene surveys that fail to capture the taxonomic and metabolic diversity of these microorganisms in soils. Here our objective was to use genome-enabled approaches to investigate methanotroph membership, distribution, and *in situ* activity across spatial and seasonal gradients in a freshwater wetland near Lake Erie. 16S rRNA gene analyses demonstrated that members of the methanotrophic *Methylococcales* were dominant, with the dominance largely driven by the relative abundance of four taxa, and enriched in oxic surface soils. Three methanotroph genomes from assembled soil metagenomes were assigned to the genus *Methylobacter* and represented the most abundant methanotrophs across the wetland. Paired metatranscriptomes confirmed that these Old Woman Creek (OWC) *Methylobacter* members accounted for nearly all the aerobic methanotrophic activity across two seasons. In addition to having the capacity to couple methane oxidation to aerobic respiration, these new genomes encoded denitrification potential that may sustain energy generation in soils with lower dissolved oxygen concentrations. We further show that *Methylobacter* members that were closely related to the OWC members were present in many other high-methane-emitting freshwater and soil sites, suggesting that this lineage could participate in methane consumption in analogous ecosystems. This work contributes to the growing body of research suggesting that *Methylobacter* may represent critical mediators of methane fluxes in freshwater saturated sediments and soils worldwide.

IMPORTANCE Here we used soil metagenomics and metatranscriptomics to uncover novel members within the genus *Methylobacter*. We denote these closely related genomes as members of the lineage OWC *Methylobacter*. Despite the incredibly high microbial diversity in soils, here we present findings that unexpectedly showed that methane cycling was primarily mediated by a single genus for both methane production ("*Candidatus* Methanothrix paradoxum") and methane consumption (OWC *Methylobacter*). Metatranscriptomic analyses revealed that decreased methanotrophic activity rather than increased methanogenic activity possibly contributed to the greater methane emissions that we had previously observed in summer months,

Received 24 May 2018 **Accepted** 1 October 2018 **Published** 6 November 2018

Citation Smith GJ, Angle JC, Solden LM, Borton MA, Morin TH, Daly RA, Johnston MD, Stefanik KC, Wolfe R, Gil B, Wrighton KC. 2018. Members of the genus *Methylobacter* are inferred to account for the majority of aerobic methane oxidation in oxic soils from a freshwater wetland. mBio 9:e00815-18. https://doi.org/10.1128/mBio.00815-18.

Invited Editor Vanessa Bailey, Pacific Northwest National Laboratory

Editor Janet K. Jansson, Pacific Northwest National Laboratory

Address correspondence to Kelly C. Wrighton, wrighton@colostate.edu.

findings important for biogeochemical methane models. Although members of this *Methylococcales* order have been cultivated for decades, multi-omic approaches continue to illuminate the methanotroph phylogenetic and metabolic diversity harbored in terrestrial and marine ecosystems.

KEYWORDS denitrification, metagenomics, metatranscriptomics, methane, methanotrophs, soil microbiology

Wetlands contribute nearly one-third of the naturally derived methane emissions globally, releasing 150 to 250 terragrams of this greenhouse gas per year (1–4). Historically, it was thought that methane was exclusively produced in anoxic horizons of wetland soils by strictly anaerobic methanogenic archaea and was subsequently consumed in oxic zones by aerobic methanotrophic bacteria, with any excess unconsumed methane potentially emitted to the atmosphere (5). These assumptions about microbial methane cycling are incorporated into biogeochemical models that estimate global terrestrial methane budgets (1, 6). However, recent reports of aerobic methanotrophy occurring in hypoxic to anoxic conditions (7–14) and of methanogenesis in oxic soils (15–17) are challenging these historical assumptions. Controlling and accurately forecasting greenhouse gas emissions require more in-depth knowledge of the factors that control natural methane production, consumption, and emission across ecosystems.

To begin to profile biological methane cycling in freshwater wetland soils, we selected the Old Woman Creek (OWC) National Estuarine Research Reserve as our model field site. This 571-acre freshwater wetland borders Lake Erie, near Huron, OH, USA, and has been shown to consistently emit methane (16, 18). During a 5-month period (June through October) in 2015, this wetland emitted approximately 129 million grams of methane and was a net carbon source for the atmosphere during the summer months (18). Previously, it was demonstrated that 40% to 90% of the methane from this wetland was produced in surface soils with oxygenated porewaters by a single methanogen species, "*Ca.* Methanothrix paradoxum" (16). While a taxonomic survey suggested that gammaproteobacterial methanotrophs, i.e., *Methylococcales*, were dominant members throughout the wetland (19), the identity and activity of these methanotrophic microorganisms were not defined along relevant temporal and spatial wetland gradients.

Here we aimed to determine the effects of soil depth, land cover, and season on methanotrophic microorganism distribution and activity in the freshwater wetland. These findings have uncovered genomic information for dominant and highly active methanotrophs within the genus *Methylobacter*, a genus that is present and active in numerous freshwater and marine sediments and in soils (14, 20–23). Given the distribution of this lineage across this wetland, including deeper soils with low dissolved oxygen (DO) concentrations, we analyzed these genomes for potential and active metabolic pathways that could support methane oxidation under hypoxic conditions. Our findings contribute to a growing body of evidence that indicates that the members of the OWC *Methylobacter* lineage are cosmopolitan and active across many freshwater and terrestrial ecosystems.

RESULTS AND DISCUSSION

Soil sampling and methane consumption potential. To understand the impact of seasonality on methanotroph distribution and activity, we sampled soils at four seasonal time points in 2014 to 2015, with sampling occurring in November 2014 representing autumn, February 2015 representing winter, May 2015 representing spring, and August 2015 representing summer. To resolve the impacts of land cover on methanotroph distribution and activity, soils were selected from three land covers ("Plant," dominated by *Typha* vegetation; "Mud," periodically exposed mud flats; "Water," permanently submerged open-water channel sediments) in a transect with locations that were equidistant from Lake Erie (Fig. 1A). At each seasonal time point, from each of the

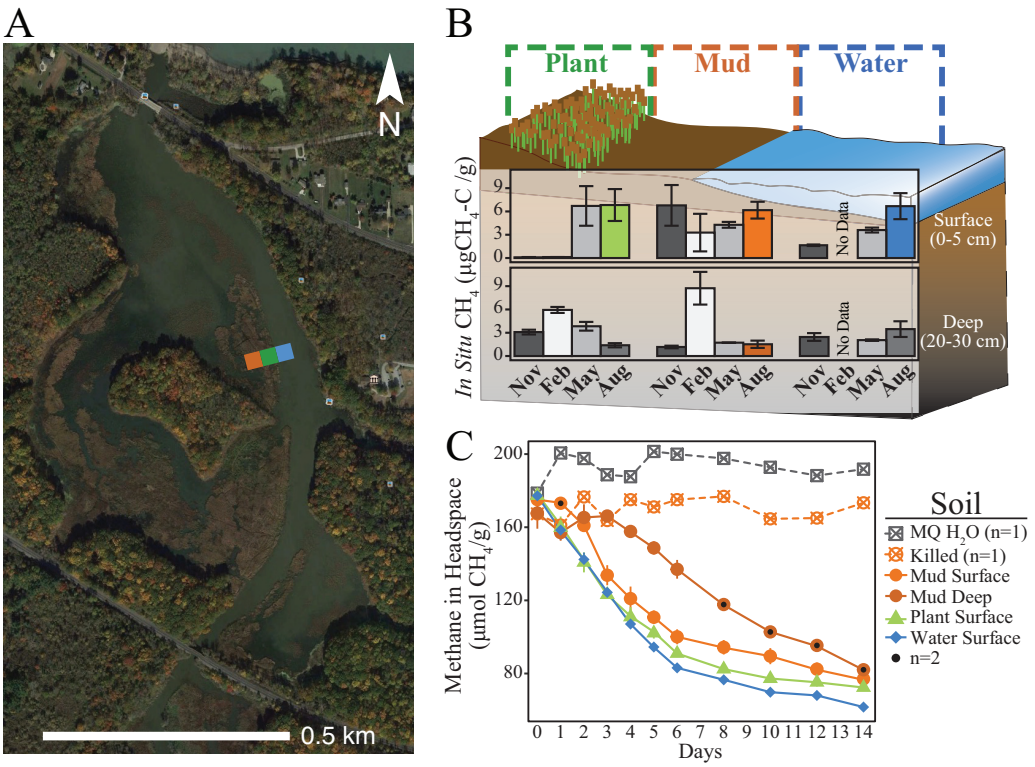

FIG 1 Overview of OWC field site and methane dynamics. (A) Old Woman Creek (OWC) National Estuarine Research Reserve is a 571-acre, NOAA-operated temperate freshwater wetland near Lake Erie in Ohio. Soils were sampled from an ecological transect composed of the following land cover types: *Typha* vegetated (Plant, green), periodically flooded mud flat (Mud, orange), and continually saturated water channel (Water, blue). We selected two soil depths as representative oxic and anoxic soil zones (0 to 5 cm, Surface; 23 to 35 cm, Deep). (B) Soil *in situ* methane concentration variation by depth and land cover type over the four sampled seasons (November 2014 through August 2015). Different months are represented as different shades of gray or are colored by land cover and depth to match the curves shown in panel C. (C) Aerobic methane consumption potential curves of surface and deep soil incubations. Points and curves are colored by the land cover type and depth in the soil column, matching the samples highlighted in panel B.

2-m² land cover plots, three cores were collected for paired 16S rRNA gene analyses. For these analyses, we focused on surface (0 to 5 cm depth) and deep (23 to 35 cm depth) soils ($n = 66$ samples), as these depths were previously demonstrated to have the most distinct bacterial and archaeal communities (19).

During the fall and summer samplings, we conducted chamber measurements, which showed that all of the studied land covers were net methane emitting (16). As a prior study demonstrated (18), eddy-covariance tower measurements showed that the greatest overall methane flux occurred during the summer months of June to September, with the greatest flux peak occurring in August. Compared to the methane emission data, the *in situ* soil methane and dissolved oxygen (DO) concentrations did not differ by season or land cover. However, the levels of both methane and DO decreased with depth across all of the land cover sites (16). The surface soils examined in August had three times more *in situ* methane (6.56 ± 0.83 versus 2.12 ± 0.47 μg CH_4-C/g) and six times more DO (79.7 ± 11 versus 12.7 ± 7 μM) than the corresponding deep soils (Fig. 1B; see also Data Set S1 in the supplemental material).

To assess the capacity for aerobic methanotrophy in our soils emitting the highest concentrations of methane, August soils were amended with methane and oxygen to measure aerobic methane consumption rates. Methane consumption in surface soils began 3 days sooner than in deep soils and continued at significantly greater rates (Fig. 1C; see also Data Set S1). Methane consumption rates in surface soils were not strongly impacted by land covers (ecological sites) but were likely strongly impacted by *in situ* methane and DO concentrations that varied with soil depth (Fig. 1B) (16). These

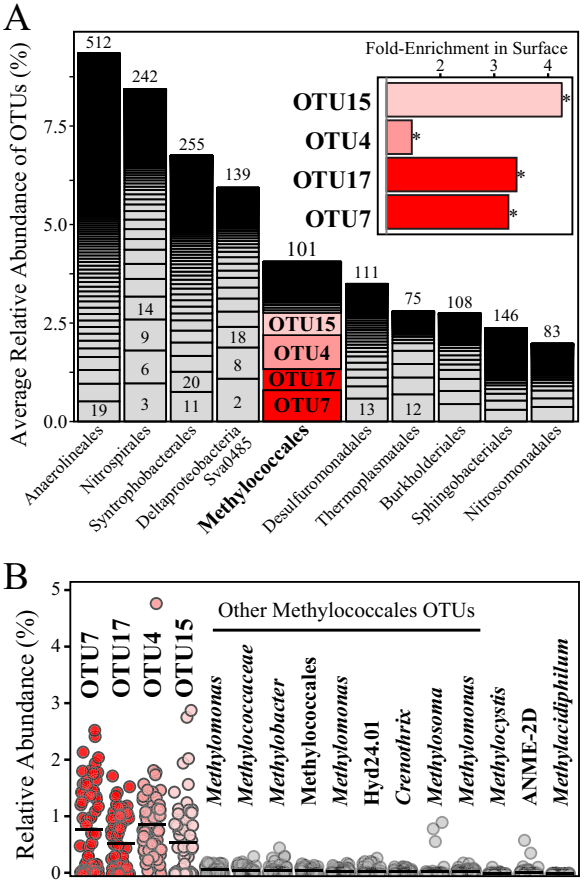

FIG 2 Relative abundances of dominant methanotrophic taxa. (A) Stacked bar chart of the 10 most abundant microbial orders in all soil samples ($n = 66$). The total number of OTUs in each order is noted above the stacked bar chart, and the relative ranks of the 20 most abundant OTUs are indicated. Four dominant *Methylococcales* OTUs are highlighted with shades of red. The inset shows fold enrichment of the dominant OTUs in surface soils over deep soils, with significant differences (analysis of variance with Tukey's range test; adjusted *P* value [*P*-adj], <0.05) indicated by asterisks. (B) The abundances of the four dominant OTUs compared to those of other detected methane-oxidizing taxa. Shown are the 10 next most abundant *Methylococcales* taxa and the most abundant OTUs of other methanotroph taxa. Dots represent individual samples, and the black bar represents the average. The four dominant OTUs were significantly more abundant (analysis of variance with Tukey's range test; *P*-adj, <0.05) than all of the other putative methanotrophic OTUs.

findings hint that methanotroph activity is likely constrained along centimeters of soil depth rather than in the distinct land covers across meters of lateral distance.

Members of the *Methylococcales* are the dominant methanotrophs in wetland soils. The members of the *Methylococcales*, methanotrophs within the *Gammaproteobacteria*, represented the fifth most abundant taxonomic order in all soils collected over four seasons, across three land covers, and at two depths (Fig. 2A). The dominance of this order was largely driven by the relative abundances of four operational taxonomic units (OTUs), which were each among the top 20 most abundant taxa of 5,662 total sampled OTUs (Fig. 2A). Here we denote these dominant methanotroph OTUs by their relative ranks in the microbial community as follows: OTU4 (GQ390219), OTU7 (ABSN01001726), OTU15 (AB5049656), and OTU17 (ABSP01000657). On the basis of the similarity of the 16S rRNA genes (V4 region), these four OTUs were most closely related to an unknown *Crenothrix* species (OTU15), *Methylobacter tundripaludum* (OTU4), and unassigned *Methylobacter* species (OTU7 and OTU17). On the basis of these partial sequences, OTU7 and OTU17 shared only ~97% identity with the closest isolated *Methylobacter* representatives *M. tundripaludum* and *Methylobacter psychrophilus*. This value is below the recently proposed species cutoff level (98%) for comparison of the

V4 regions within members of the *Methylococcaceae* (24); however, we note that caution must be used in interpreting phylogenetic relationships with a single and, especially, partial marker genes.

On average, these four OTUs were each significantly more abundant than all of the OTUs of other known methane-oxidizing taxa (Fig. 2B). Corroborating the methane consumption potential patterns (Fig. 1C), these four OTUs were up to 4-fold more abundant in surface soils than in deeper soils (Fig. 2A, inset) but were not significantly different between land covers or seasons (see Fig. S1A in the supplemental material). Furthermore, the relative abundances of three of these OTUs (OTU7, OTU15, and OTU17) were positively correlated to DO concentrations in the soils ($P < 0.02$) (Fig. S1B). Our findings, along with prior publications from studies of this wetland using data sampled more than a year earlier than here (19), imply that members of the *Methylococcales* are the dominant methanotrophs in surface soils and likely represent critical components of microbial methane cycling in this wetland.

Discovery and phylogenetic placement of new *Methylococcales* genomes. To better ascertain the metabolic potential of these dominant *Methylococcales* species in the surface soils, metagenomic sequencing was performed on one representative surface (0 to 5 cm depth) soil from each land cover category (plant, mud, and water) at two time points representing plant senescence in late fall (November 2014) and peak primary productivity (August 2015) ($n = 6$). While we observed no significant differences in methanotroph 16S rRNA gene relative abundances across these gradients, we hypothesized that metagenomics may capture species- or strain-level variations occurring along spatial or seasonal gradients that were not made apparent by 16S rRNA gene sequencing. Additionally, by sequencing metagenomes across various seasons and sites, we expected to increase the likelihood of sampling near-complete genomes from these complex soils, a feature necessary to support our metatranscriptomic analyses.

Metagenomic sequencing yielded 304 Gbp of Illumina HiSeq data. *De novo* assembly of these metagenomes resulted in approximately 3.8 Gbp of genomic information contained in scaffolds greater than 5 kb in size. Using a combination of automated binning and manual binning (see Text S1 in the supplemental material), we recovered four genomic bins likely belonging to methanotrophic bacteria, as determined by the presence of key methanotrophy functional genes and genes with taxonomic affiliation to members of the *Methylococcales*. In accordance with our 16S rRNA gene data (Fig. 2), we did not recover bins for other bacterial or archaeal methanotrophs.

The reconstructed methanotroph genomes were estimated to be up to 97% complete (65%, 74%, 81%, and 97%), all with overages of less than 4% (Data Set S1). All of these genomes were from the November metagenomes and would be classified as medium quality using the recently proposed Genomic Standards Consortium benchmarks (25). The August metagenomic sequencing did not yield methanotroph genomes that were greater than 50% complete but did yield other complete genomes, demonstrating that differences in community structure impacted genome recovery.

We recovered three closely related genomes from the different land covers (including genomes NSM2-1 [mud], NSO1-1 [water], and NSP1-1 [plant]), which we conclude are likely members of the same species (discussed below). From one of these genome bins (NSP1-1 scaffold_2426), we recovered a single 404-bp 16S rRNA gene fragment. This gene fragment was 100% identical to all three near-full-length EMIRGE (~900-bp) (26) sequences generated from unassembled reads from the same November metagenomes where these genomes were recovered (Data Set S1).

Comparison of these near-full-length sequences and the 16S rRNA gene sequences from other *Methylococcales* genomes showed that our recovered metagenome 16S rRNA sequences were closely related strains (>99.8% identity; see Data Set S1) within the genus *Methylobacter*. We, and others (11, 14, 27–30) have noted that the genus *Methylobacter* is not monophyletic and instead contains two (possibly genus-resolved) clades (Fig. S2). Clade 1 contained *Methylobacter* species *M. whittenburyi*, *M. marinus*, *M. luteus*, and *M. BBA5.1*, while clade 2 contained *Methylobacter tundripaludum* and *M.*

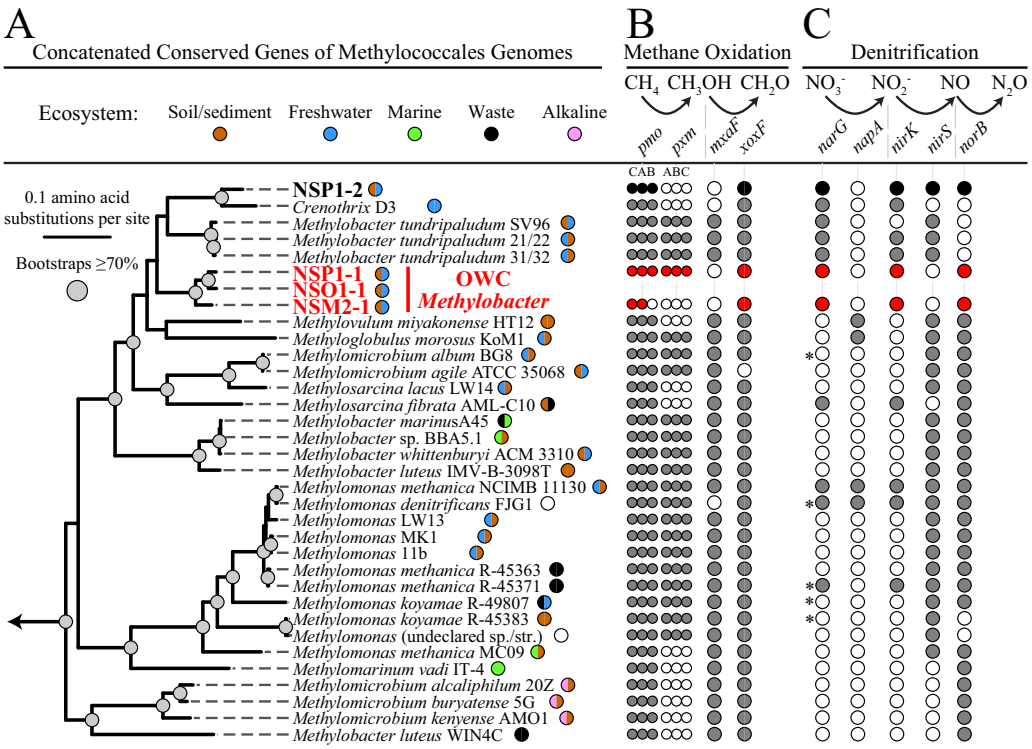

FIG 3 Phylogenetic placement of novel genomes and overview of methane and dissimilatory nitrate reduction metabolisms. (A) Maximum likelihood tree constructed from 21 concatenated universally conserved single-copy and ribosomal protein genes (3,270 amino acids [aa]), rooted to *Nitrosococcus*. Our four genomes represent two novel lineages (Text S1): OWC *Methylobacter* (red) and NSP1-2 (black). Ecosystem types are indicated by colored circles next to the genome name. (B) Inventory of the presence and types of particulate methane monooxygenase (*pmo*), *pmo*-like (*pxm*), and methanol dehydrogenase (*mxaF*, *xoxF*) genes in *Methylococcales* genomes (Data Set S1). (C) Dissimilatory nitrate and nitrite reduction marker genes found in *Methylococcales* genomes. Gene expression or biochemical transformations demonstrating dissimilatory nitrate or nitrite reduction are indicated by the asterisks (Data Set S1). Inventories are not shown for NSO1-1 due to lack of core genes.

psychrophilus species. A phylogenetic analysis of our three near-full-length representative OWC *Methylobacter* sequences reconstructed using EMIRGE grouped these genomes with the clade 2 *Methylobacter* genus but were divergent from *M. tundripaludum* or *M. psychrophilus* sequences (Fig. S2).

Additional phylogenetic analyses using single and concatenated housekeeping genes, as well as single functional genes, confirmed the placement of our genomes within clade 2 and yet also showed that the OWC genomes were divergent from the currently isolated species (*M. tundripaludum* and *M. psychrophilus*). For instance, a concatenated phylogenetic tree composed of 14 ribosomal proteins and 7 universally conserved single-copy marker genes that were present in our *Methylococcales* genomes and in 53 other sequenced *Methylococcales* genomes (Fig. 3A) revealed that three of these OWC genomes formed a well-supported lineage that was most closely related to but likely divergent from *M. tundripaludum*. The results from our *pmoA* gene (Fig. S3), methanol dehydrogenase (Fig. S4), and whole-genome-wide nucleotide and amino acid comparisons (Text S1) also support the characterization of our genomes as members of *Methylobacter* clade 2 and, potentially, as a separate species-level lineage within this genus. We conservatively refer to these genomes at the genus level, denoting that the members of the OWC *Methylobacter* represent a lineage of *Methylobacter* clade 2.

A fourth recovered *Methylococcales* genome (NSP1-2) was phylogenetically distinct from the three OWC *Methylobacter* genomes (NSM2-1, NSO1-1, and NSP1-1) (Fig. 3). This more divergent genome, which lacked a 16S rRNA gene recovered from the genome bin, lacked confident taxonomic assignment using our concatenated marker

gene phylogenies (Fig. 3A) and *pmoA* phylogenies (Fig. S3; see also Text S1). But this genome appeared most closely related to *Crenothrix* sp. D3 by the use of multiple phylogenetic markers, including concatenated and single-copy marker genes (Fig. 3A; see also Fig. S3 and Text S1). Given this lack of taxonomic congruency and the inability to link to our 16S rRNA gene amplicon data, we focus our primary analyses in the manuscript on the OWC *Methylobacter* clade 2 lineage genomes (NSM2-1, NSO1-1, and NSP1-1).

The discovery of phylogenetic novelty is consistent with recent sampling of the uncultivated diversity within the *Methylococcales* over the past few years. Much of this new insight can be attributed to the reconstruction of genomes from metagenomes obtained from diverse environments (Fig. 3A). This includes the recovery of genomes representing *Methylothermaceae* sp. B42 genome from deep-sea hydrothermal vents (12), the OPU3 genome from marine oxygen minimum zones (10), *Crenothrix* sp. D3 genome from lacustrine waters (11), and Upland Soil Cluster γ from Antarctic cryosols (31). Although *Methylococcales* species have been cultivated for decades, genomes reconstructed from metagenomes continue to illuminate the methanotroph genome diversity present across terrestrial and marine ecosystems.

OWC *Methylobacter* and the NSP1-2 genomes encode mechanisms to putatively withstand oxygen limitation. All four of our *Methylococcales* genomes have the essential genes for methane oxidation, including genes encoding particulate methane monooxygenase (*pmo*) (Fig. 3B) and the methanopterin-linked C1 transfer pathway and formate dehydrogenase and the genes necessary for the carbon assimilation via the ribulose monophosphate pathway (RuMP) cycle (Data Set S1). Despite the prevalence of phylogenetic marker genes in the NSO1-1 genome (indicated by its inferred 81% completion), we noted that many core metabolic genes were not recovered in this genome bin. Because we cannot easily distinguish ineffective binning in this metagenome-reconstructed genome from the absence of genes, we do not include a summary of the metabolic potential for this genome in Fig. 3, but the metabolic data for this genome were inventoried (Data Set S1).

Our four genomes encode canonical methane oxidation, aerobic electron transport chain components, and formaldehyde metabolism conserved in other *Methylococcales* (Data Set S1). We failed to detect a soluble methane monooxygenase gene (*smo*) in any of our four genomes; OWC *Methylobacter* genomes likely have the sequence-divergent *pmo* gene (*pxm*) (Fig. 3B; see also Data Set S1). Our reconstructed genomes contained *xoxF5*-type methanol dehydrogenases, but we failed to detect the traditional *mxaF*-type methanol dehydrogenase gene in our genome bins (Fig. 3B; see also Fig. S4) or in any of the unbinned scaffolds in our metagenomic data. Consistent with our findings, the lack of *mxaF* has been reported in methylotrophic microorganisms found in a variety of habitats (10, 32–38). However, we recognize that caution must be used for inferring metabolic capacity on the basis of the absence of genes in genomes derived from metagenomic reconstruction. We also recovered high-affinity cytochrome *bd* ubiquinol oxidase (*cyd*) and Na(+) translocating NADH-quinone oxidoreductase (*nqr*) genes. The functions of some of these genes in methane oxidation are still uncertain, but they may mediate responses to fluctuating oxygen conditions (*cyd*) (9, 39, 40), alter metal requirements or interactions with other community members (*xoxF*) (32, 33, 41), or provide alternative routes for ATP generation via a sodium motive force (*nqr*) (12, 42).

On the basis of recent expansions of the metabolic capacity of *Methylococcales* genomes (43, 44), we inventoried the denitrification potential in our genomes and across the order (Fig. 3C; see also Data Set S1). Our analyses expanded upon research by Padilla et al. indicating that inventoried nitrate reduction potential in 26 members of this order (10). Here we included 31 additional genomes, with a focus on *Methylobacter* members, and also included a survey of methane monooxygenase and methanol dehydrogenase diversity in this order (Fig. 3B; see also Data Set S1). Few of these features appear strongly phylogenetically conserved at the genus level, but major functional differences among *Methylomicrobium* and *Methylobacter* groups were observed. For example, *Methylomicrobium* species most similar to *Methylosarcina* pos-

sessed *pxm* whereas the other *Methylomicrobium* species did not (Fig. 3A), and clade 2 but not clade 1 *Methylobacter* species have the capacity for dissimilatory nitrate reduction (Fig. 3C; see also Fig. S5 and Data Set S1). In addition to clade 2 *Methylobacter* species, our analyses revealed the presence of dissimilatory nitrate reduction pathways in over one-third of the sequenced *Methylococcales* genomes (23/57 analyzed) (Fig. 3C; see also Data Set S1). Furthermore, nearly two-thirds of these genomes contained a form of dissimilatory nitrite reduction and nitric oxide reductase (40/57 with *nirK* or *nirS* and 41/57 with *norB*; see Data Set S1). Both of the metabolically more complete OWC *Methylobacter* genomes (NSM2-1 and NSP1-1) and the divergent genome (NSP1-2) contained key functional genes for dissimilatory reduction of nitrate (*narG*), nitrite (*nirK*), and nitric oxide (*norB*) (Data Set S1).

While some of the recent discoveries of denitrification pathways encoded by *Methylococcales* have noted that the *narG* genes were most phylogenetically related to other bacterial lineages (10, 12), our OWC *Methylobacter narG* genes formed a monophyletic clade with sequences with other *Methylococcales* genomes (Fig. S5C). Moreover, the OWC *Methylobacter narG* sequences contained the necessary residues for substrate and cofactor binding (Fig. S5A) (45) and were structurally homologous to the NarG used for denitrification by *Escherichia coli* (Fig. S5B). The net impact of this nitrogen-based metabolism is uncertain, as our analyses showed that all of the genomes in our study, and others within this family, lack the capacity to reduce nitrous oxide (*nosZ*). Thus, this proposed denitrification activity could potentially generate nitrous oxide, emitting a more potent greenhouse gas than carbon dioxide or methane (46). While expression of *Methylococcales* denitrification pathways has been observed under laboratory conditions (7–9) and in hypoxic marine systems (10), field-scale studies determining the extent and climatic tradeoffs of this process in terrestrial systems are currently not known.

Given the detection of OWC *Methylobacter* OTUs (OTU7 and OTU17) in deeper hypoxic or anoxic soils (Fig. 2A, inset) (19), we examined our genomes for other mechanisms that would enable greater tolerance of low oxygen and methane concentrations. Prior publications have reported microaerobic fermentation by *Methylomicrobium buryatense*, another member of the *Methylococcaceae*. In this fermentative metabolism, transformation of formaldehyde through the RuMP and glycolysis to produce pyruvate ultimately leads to mixed acid fermentation products and ATP (11, 47, 48). Similar metabolic capabilities were detected in OWC *Methylobacter* genomes and NSP1-2 (Text S1; see also Data Set S1). However, we acknowledge that it is challenging to infer facultative fermentative metabolism from genomes corresponding to respiratory capacities. In a second example, bidirectional [NiFe] hydrogenase (*hox*) genes were harbored in these genomes, suggesting that hydrogen may be used as an electron donor, as previously reported for more distantly related methanotrophs (49, 50). Lastly, we found hemerythrin genes in our genomes that could be involved in responding to variations in oxygen concentrations or in shuttling oxygen directly to the particulate methane monooxygenase enzyme complex (Text S1) (51–56). In support of the idea of these roles, it was recently shown that the presence of *Methylomicrobium buryatense* increased the expression of *hox* and hemerythrin genes in response to oxygen starvation (48). From our work and that of others performed across a range of ecosystems, there is increasing evidence that members of the aerobic *Methylococcales* encode multiple mechanisms to sense and maintain methane consumption during oxygen limitation. We posit that this versatile genetic repertoire involved in responses to changes in oxygen concentrations may contribute to the cosmopolitan distribution of these taxa observed under various redox conditions.

OWC *Methylobacter* genomes are the most active methanotrophs in the oxic wetland soils. To examine methanotrophic activity among the land covers during different seasons, metatranscriptomic sequencing was performed on triplicate surface soils from the plant and mud land covers in November and August ($n = 12$), yielding 462 Gbp of data (16). OWC *Methylobacter* genomes' *pmo* genes were among the top 3% most highly transcribed genes in the soils (Fig. 4A) and accounted for nearly 98% of the

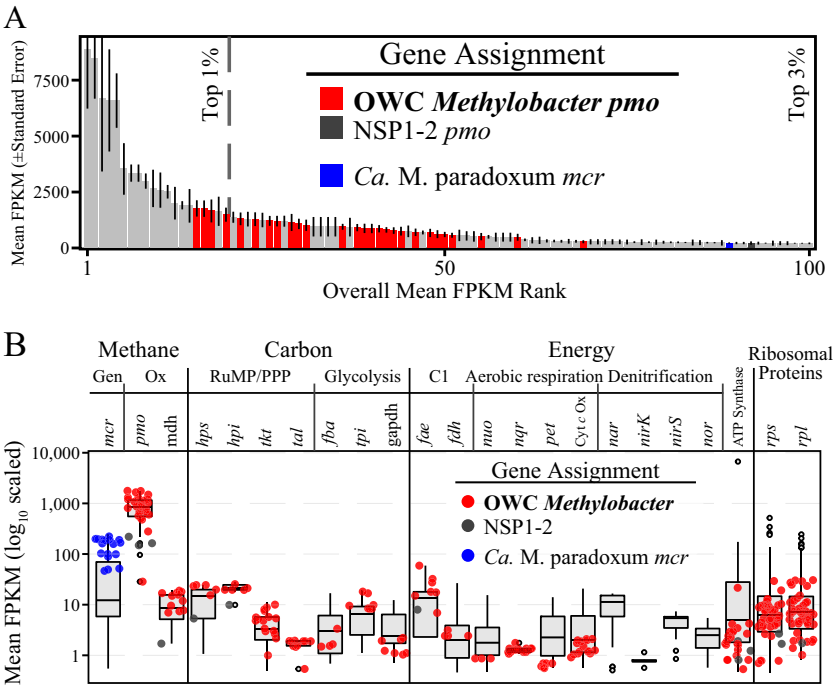

FIG 4 OWC *Methylobacter* and NSP1-2 gene expression in surface soils. (A) Rank abundance curve of the top 100 annotated genes by average normalized gene expression (FPKM [fragments per kilobase of exon per million mapped reads]) in surface soils ($n = 12$). The approximate positions of the top 1% and 3% of the 22,219 genes with detectable transcripts are indicated. (B) Box plots of the mean expression levels of representative genes from core methane (Gen, generation; Ox, oxidation), carbon (RuMP/PPP, ribulose monophosphate pathway or pentose phosphate pathway), and energy generation (C1, C1-transfer) pathways and bulk ribosomal protein gene transcript abundances. The data from the genes assigned to OWC *Methylobacter* and NSP1-2 and the *mcr* gene of "*Ca.* Methanothrix paradoxum" were averaged across all 12 samples and overlaid onto the box plots (colored circles; see Data Set S1). Abbreviations are as follows: *mcr*, methyl coenzyme-M reductase; *pmo*, particulate methane monooxygenase; mdh, methanol dehydrogenase; *hps*, hexulose-phosphate synthase; *hpi*, hexulose phosphate isomerase; *tkt*, transketolase; *tal*, transladolase; *fba*, fructose 1,6-bisphosphate aldolase; *tpi*, triose phosphate isomerase; gapdh, glyceraldehyde phosphate dehydrogenase; *fae*, formaldehyde-activating enzyme; *fdh*, formate dehydrogenase; *nuo*, NADH dehydrogenase; *nqr*, Na(+)-translocating NADH:ubiquinone oxidoreductase; *pet*, ubiquinol cytochrome *bc* reductase; Cyt c Ox, cytochrome *c* oxidase; *nar*, respiratory nitrate reductase; *nirK*, copper-containing nitrite reductase; *nirS*, cytochrome *cd*$_1$ nitrite reductase; *nor*, nitric oxide reductase; *rps*, small subunit ribosomal protein; *rpl*, large subunit ribosomal protein.

pmoA transcripts (Fig. 4B). The remaining ~2% of the *pmoA* transcripts were assigned to the divergent NSP1-2 genome (Fig. S6A). Ribosomal protein gene transcript abundances confirmed that OWC *Methylobacter* methanotrophs were some of the most active microorganisms within the surface soil community (Fig. 4B) and that the high transcript abundances were not an artifact of *pmoA* transcript stability. In summary, our data identified members of the OWC *Methylobacter* lineage as the most active methanotrophs in these surface soils.

Transcripts for pathways downstream of methane oxidation, e.g., pathways corresponding to methanol dehydrogenase and assimilatory and dissimilatory formaldehyde metabolisms, glycolysis/gluconeogenesis, and aerobic respiration, were also detected for the OWC *Methylobacter* genomes (Fig. 4B). Genes that were notably absent in our metatranscriptomic analyses included genes corresponding to pathways supporting methane oxidation under hypoxic conditions, despite detectable transcripts for a variety of anaerobic metabolic pathways employed by other microorganisms. For example, we did not detect transcripts for OWC *Methylobacter*-catalyzed denitrification (Fig. 4B), the high-affinity terminal oxidase (*cyd*), putative microaerobic fermentation to lactate or ethanol, or hemerythrin by OWC *Methylobacter* in these oxic surface soils (Data Set S2). It is possible that the dissolved oxygen levels in the surface soils (79.7 ± 11.3 μM) precluded the need for oxygen-conserving metabolisms. Ongoing

transcript measurements along finely resolved depths will better evaluate the potential activity of these oxygen-conserving mechanisms employed by OWC *Methylobacter* in these soils.

A quantitative analysis of the *pmoA* genes recovered in our genomes across wetland gradients revealed a putative seasonal response. While the transcript abundances of OWC *Methylobacter pmoA* genes did not significantly differ between plant and mud land covers in a season, we detected an approximately 4.5-fold decrease in relative transcript abundances from November to August (Fig. S6B). A similar trend was observed for most OWC *Methylobacter* genes (Data Set S2), suggesting that overall methanotrophic metabolism, and not just that of *pmoA* transcripts, was reduced in August. We confirmed that this decrease in inferred activity in August occurred after normalization and thus was not due to seasonal variations in metatranscriptomic sequencing (16). We additionally verified that the decrease in August was not due to a shift in the active methane-oxidizing bacteria by mapping these metatranscriptomes to a database containing 99 *pmoA* genes from sequenced genomes (53 *Methylococcales*, 30 Rhizobiales, 13 *Methylacidiphilum*, and 3 "*Candidatus* Methylomirabilis" genomes, not shown). We entertain the idea that perhaps the OWC *Methylobacter* methanotrophs are cold adapted, similarly to what has been reported for other related *Methylobacter* clade 2 members (14, 21, 29, 57–67). In contrast to the methanotroph activity primarily exhibited by OWC *Methylobacter*, levels of transcripts of normalized methyl coenzyme A reductase (associated with *mcrA*, the functional marker for methanogenesis) from the dominant methanogens did not significantly change between November and August (Fig. S6C) (16). This transcript pattern provides evidence that reduced methanotrophic activity, rather than increased methanogenic activity, may contribute to the increased methane emissions reported in summer months (18). Consequently, this diminished methanotroph activity may also contribute to the ~2.3-fold-greater *in situ* methane concentrations observed in August surface soils (Fig. 1B).

We previously reported that methane is produced in bulk oxygenated surface soils and that the production is largely mediated by a single methanogen species, "*Ca.* Methanothrix paradoxum" (16). Here we show that OWC *Methylobacter* OTUs (OTU7 and OTU17) and the OTU representing the methanogen "*Ca.* Methanothrix paradoxum" (CU916150) significantly co-occurred in both the mud land cover and plant land covers ($P < 0.02$). In the mud land cover, where a disproportionately large quantity of methane is released (18), transcript abundances of OWC *Methylobacter pmoA* and "*Ca.* Methanothrix paradoxum" *mcrA* genes were also highly correlated ($P < 0.02$). This suggests that these two dominant methane-cycling microorganisms may form a mutualistic relationship, where the methanogenesis by "*Ca.* Methanothrix paradoxum" that we presume occurs in anoxic microsites (16) subsequently feeds methane oxidation by OWC *Methylobacter* in peripheral oxygenated zones. Methane oxidation leads to further local oxygen scavenging, providing a positive-feedback loop to sustain anaerobic methanogenesis in anoxic microsites within bulk-oxygenated surface soils. Furthermore, dominance by a single methanogen species and a single methanotroph species has been observed in other Northern latitude hydric soils such as thawing permafrost (14, 66–68). Therefore, despite the extremely high richness and strain diversity present in soils, parameterizing microbial methane cycling on the ecosystem scale may be simplified to correspond to several tractable microorganisms.

OWC *Methylobacter* species are present in other methane-emitting, hydric soil ecosystems. In an effort to distinguish the global distribution of the OWC *Methylobacter* lineage from that of other closely related *Methylobacter* clade 2 members (*M. tundripaludum* and *M. psychrophilus*), we mined publicly available soil and freshwater metagenomic, metatranscriptomic, and clone library databases using *pmoA* genes from OWC *Methylobacter*. We identified 218 of the sequences most closely and significantly affiliated with OWC *Methylobacter* but not with other clade 2 *Methylobacter* members among 71 different sequencing data sets (Fig. S7; see also Data Set S1). Samples containing members closely related to OWC *Methylobacter* were from nine different freshwater and soil locations throughout the United States, Canada, Europe, Russia,

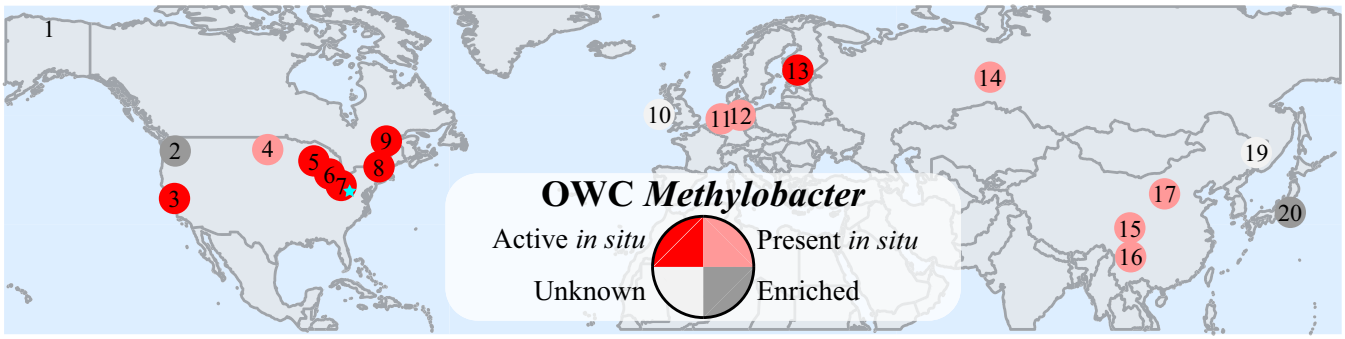

FIG 5 Distribution of OWC *Methylobacter pmoA* genes detected in publicly available sequencing databases. Numbers indicating specific locations are indicated in Data Set S1, and the shading indicates the type of sequencing performed in the study as follows: Active *in situ*, detected in environmental metatranscriptomes; Present *in situ*, detected in environmental metagenomes or clone libraries; Enriched, detected in incubation sequencing studies. NSP1-2 was found at the locations numbered 1, 2, 5, and 7. The cyan star indicates the bubble representing this study. A representation of the sequences assigned to OWC *Methylobacter* and NSP1-2 is visualized in Fig. S7, and the full list of accession numbers and the accompanying metadata are available in Data Set S1.

China, and Japan (Fig. 5; see also Fig. S7 and Data Set S1). OWC *Methylobacter pmoA* genes were also detected in seven metatranscriptomic studies, suggesting that members of this clade may be active methanotrophs in other ecosystems (Fig. 5; see also Fig. S7 and Data Set S1). These closely related OWC *Methylobacter* genes were found in samples that included Lake Washington sediments where methylotrophic metabolism has been extensively investigated (20, 69) and samples from prairie potholes in North Dakota that showed some of the highest recorded levels of methane fluxes (70) (Data Set S1). Notably, both of the dominant methane-cycling microorganisms present in the OWC soils, "*Ca.* Methanothrix paradoxum" and OWC *Methylobacter*, were present and active in a restored wetland in the San Joaquin Delta in California (16, 71) (Data Set S1), signifying that these two lineages may operate together in other hydric soil systems.

Summary. Microorganisms inhabiting permafrost, wetlands, and soils in the Northern hemisphere are predicted to be critical for terrestrial-atmospheric methane exchange (6, 14). Here we reconstructed three genomes belonging to the genus *Methylobacter*. From paired metagenomics and metatranscriptomics data, we infer that this OWC *Methylobacter* lineage represents some of the most abundant and active microorganisms across spatial, depth, and seasonal soil gradients. We demonstrated that the level of transcripts indicative of methane consumption activity had decreased 4.5-fold in our summer samples, potentially contributing to the site-wide increase in the levels of methane surface soil concentrations and emission during this time. Genes and transcripts affiliated with OWC *Methylobacter* were detected in other methane-emitting hydric soils and sediments from North America, Europe, Russia, and Asia. Our results indicate that members of clade 2 *Methylobacter* may be important, cosmopolitan methanotrophs present and active across many ecosystems.

MATERIALS AND METHODS

Field sample collection. Old Woman Creek National Estuarine Research Reserve (41°22′N 82°30′W) is located at the southern edge of Lake Erie. The 571-acre freshwater wetland co-operated by the National Oceanic and Atmospheric Administration (NOAA) and the Ohio Department of Natural Resources is one of 28 coastal sentinel research sites. We collected soils and greenhouse gas emissions during November 2014 (fall), February 2015 (winter), May 2015 (spring), and August 2015 (summer). Greenhouse gasses were collected and analyzed as previously described (16, 18). Four or more soil cores were extracted using a modified Mooring system corer from ~2 m^2 of soil at three distinct land covers (18, 72–74): emergent vegetated *Typha* (plant), periodically flooded mud flat (mud), and permanently submerged channel sediments (water). In February, six samples from the water channel could not be collected due to frozen, unstable conditions; hence, the total number soil samples analyzed here was 66 and not 72. Cores were stored on ice in the field until hydraulic extrusion and subsampling were performed (~2 h). DO was measured along the vertical profile in 5-cm increments using an oxygen dipping probe (DP-Pst3) received with a standalone fiber optics Fibox 4 meter (Presens) (16).

Soils were subsectioned into two depths, 0 to 5 cm (surface) and 23 to 35 cm (deep) below the soil surface, and the samples were allocated into sterile WhirlPak bags for biological and geochemical measurements. Soils used for geochemical measurements were stored at 4°C, and soils used for DNA extraction and RNA extraction were stored at −20°C and −80°C, respectively. The methods used to

quantify soil and pore water geochemistry were previously described in detail by Angle et al. (16). *In situ* methane concentrations were measured using a Shimadzu GC-2014 chromatograph.

Methane consumption potential. Analyses of the aerobic methane consumption potentials of August soils were conducted using a modified version of an experiment previously described by Chan and Parkin (75). Soils from the surface of each land cover and deep soils from the mud land cover collected in August were selected. Soils (5 g) were added to amber vials (35 ml) and were sparged with N_2 gas immediately. Autoclaved MilliQ (5 ml) was added to improve homogeneity. The headspace of the vials was flushed with 120 ml of air that had been filtered using a 0.2-μm-pore-size filter, and then 2.5 ml (~10% of the headspace) was removed and replaced with methane. One additional processed surface soil from the mud land cover was autoclaved three times for 20 min each time to serve as a killed control and to account for nonbiological soil methane oxidation. Additionally, one vial containing only 10 ml of sterile MilliQ water was used as a negative control. Methane in the headspace was sampled daily for 1 week and then every other day for the following week. The headspace volume (5 ml) was injected into a Shimadzu GC-2014 chromatograph, and the volume was replaced with a methane-air mixture (approximately 10:90). Consumption rates were calculated from empirically determined linear portions of each curve (see Data Set S1 in the supplemental material).

Extraction of nucleic acids and preparation of sequencing data for analyses. 16S rRNA gene analyses were performed on surface and deep soils from triplicate cores from each land cover (plant, mud, and water) over four seasons (November, February, May, and August) ($n = 66$). The V4 regions of the 16S rRNA genes were sequenced at Argonne National Laboratory's Next Generation Sequencing Facility to generate 2-by-251-bp paired-end reads using a single lane of an Illumina MiSeq system (76). Reads were processed using QIIME to generate OTUs and calculate relative abundances (77). To identify the most abundant taxonomic groups (Fig. 2A), the relative abundances of each OTU were averaged over all samples, and the results were then summed according to the unique bacterial and archaeal orders detected. Fold enrichments on each wetland ecological gradient were calculated by comparing the mean relative abundances of the individual OTUs between land covers or seasons.

For metagenomics, we selected surface soils from a single representative core from each of the three land covers (plant, mud, and water) in two seasons (November and August) ($n = 6$). For metatranscriptomics, we performed RNA extractions from each triplicate core and from two land covers (plant and mud) in both seasons ($n = 12$). The nucleic acid extraction protocol was explained previously (16). Briefly, DNA was extracted from each soil sample using MoBio PowerSoil DNA isolation kits, while RNA was extracted using MoBio Powersoil total RNA isolation kits, both performed following the instructions of the manufacturer. DNA was removed from RNA samples using a DNase Max kit (MoBio), and the results were verified by the use of SuperScript III first-strand synthesis (Invitrogen) and PCR.

Genomic DNA was prepared using a TruSeq Rapid Exome Library Prep kit (Kapa Biosystems), and metagenomes were sequenced at The Ohio State University (November) and the Joint Genome Institute (August) using an Illumina HiSeq system. The methods were described previously (16, 77), but briefly, reads for each metagenome were individually assembled *de novo* using IDBA-UD (78), while gene calling and identification were performed by bidirectional querying of multiple databases (79). Scaffolds of >2 kbp in length were binned by tetranucleotide frequencies using emergent self-organizing maps (ESOM) (79, 80) and were further manually curated by GC, coverage, and taxonomic affiliation (see Text S1 in the supplemental material). Completion of each genome was estimated by analysis of the presence of 31 conserved bacterial genes that generally occur in single copy within microbial genomes by the use of Amphora2 (81). Unassembled reads were used to reconstruct near-full-length 16S rRNA gene sequences using EMIRGE (26).

RNA was prepared at JGI using a TruSeq Stranded Total RNA LT Sample Prep kit (Kapa Biosystems), which includes rRNA depletion and cDNA synthesis steps, and was sequenced using an Illumina HiSeq system to generate 2-by-150-bp paired-end reads. Those reads were quality checked and trimmed in the same manner as the metagenomic reads. Reads were mapped to a database containing genes on assembled scaffolds that were >1 kbp from all six metagenomes using Bowtie2 (82), allowing a maximum of 3 mismatches (16). Transcript abundances were corrected for multimapping and normalized by gene length and library size by the use of Cufflinks (83), resulting in units of fragments per kilobase per million mapped reads (FPKM). Separate read mapping to a database of 99 *pmoA* genes, from sequenced genome representatives of *Methylococcales*, *Rhizobiales*, *Methylacidiphilum*, and "*Ca.* Methylomirabilis" retrieved from the Integrated Microbial Genomes and Metagenomes website (IMG/M) or NCBI (see below), was performed in the same manner.

Phylogenetic analyses of the genomes and marker genes of methanotroph genomes. Publically available *Methylococcales* genomes were mined in September of 2017 from the Integrated Microbial Genomes and Metagenomes website (IMG/M [https://img.jgi.doe.gov/]) (84). These genomes were supplemented with that of *Crenothrix* sp. D3 (taxonomy identifier [ID] 1880899) (11) obtained via the National Center for Biotechnology Information (NCBI [https://www.ncbi.nlm.nih.gov/]) and with OPU3 extracted from the supplemental material provided by Padilla et al. (10). *Nitrosococcus* species were used as a phylogenetic root because they are members of the *Gammaproteobacteria* and their hallmark ammonia monooxygenase (*amo*) gene shares evolutionary history with *pmo* (40), allowing the same root microorganisms to be used in all phylogenetic analyses, except analyses of methanol dehydrogenase. Genes were identified in these genomes using BLASTp with an E value threshold of 1e−20, and the resulting sequences were manually curated to remove false positives by analysis of operon architectures, sequence alignment, and FastTree topologies (85). Genes on unbinned contigs were assigned to OWC *Methylobacter* or NSP1-2 genomes for transcriptomic analyses by determinations of shared identity levels

of >95% over a minimum of 1,000 bp. The affiliations of the genes of interest on these contigs were additionally verified by alignment with the matching genes in the genomes.

For each analysis, genes were aligned using MUSCLE 3.8.31 (86) and were manually curated in Geneious 7.1.9 (87) to remove end gaps and to adjust poorly aligned regions or sequences prior to concatenation performed using Geneious. Maximum likelihood phylogenetic trees were generated using RAxML 8.3.1 (88) with 100 bootstraps.

Methylococcales 16S rRNA gene sequences were retrieved from SILVA (https://www.arb-silva.de/) small-subunit (SSU) 128 RefNR (89) and were supplemented with genes in sequenced genomes in IMG/M. This reference database was dereplicated manually by keeping only those sequences present in genomes of isolates or reconstructed from metagenomes and eliminating multicopy rRNA genes (except those of *Crenothrix polyspora*). The 16S rRNA gene phylogeny was generated using the GAMMAGTR substitution model.

We sought to confirm the identities of the *pmo* and *pxm* genes present in our methanotroph genomes by analysis of branching patterns in addition to conserved operon architecture (40). Operon architectures were visualized on IMG/M using the "Gene Neighborhoods" tool or by scanning the gene orders for OPU3 and *Crenothrix* sp. D3. The phylogenies of *pmoA*, *pmoB*, and *pmoC* were aligned individually using the respective *amo* genes as outgroups. Unbinned *pmo* and *pxm* genes were assigned to OWC *Methylobacter* or NSP1-2 by a combination of overall shared identities and phylogenetic groupings (Data Set S1). Nucleotide phylogeny data were generated using the GAMMAGTR model with Jukes-Cantor correction (28), and the amino acid phylogeny was constructed using the PROTGAMM AWAG substitution (11).

For concatenated phylogenetic analyses using universally conserved single-copy genes (90) and ribosomal protein genes (91), all protein sequences were individually aligned and curated and then concatenated into a single alignment using Geneious. The genes used are described in Data Set S1. All of the genes were present in approximately single copy in all four of our reconstructed genomes, and reference genomes were included only if they were missing a maximum of one gene. The resulting tree (Fig. 3A) was generated using the PROTCATLG model (77, 91). However, we note that the topology of this tree was maintained regardless of the gene concatenation order, the addition or subtraction of genes and genomes, the substitution model, and similarity to the results of single-gene analyses (i.e. ribosomal protein S3; not shown).

In order to determine the type(s) of methanol dehydrogenase encoded by OWC *Methylobacter* and NSP1-2, we compared their methanol dehydrogenase amino acid sequences to those published in Taubert et al. (92). We included additional *Methylococcales* species in order to inventory the methanol dehydrogenase types in this order, as this has not been previously reported (32, 41, 93). The phylogeny (see Fig. S4 in the supplemental material) was generated using the substitution model determined by ProTest (94). Unbinned portions of the metagenomes were mined for *mxaF*-type and *xoxF*-type methanol dehydrogenases (except those that were associated with fewer than 300 amino acids, which were removed) via BLAST and annotation searches and aligned using MUSCLE software, and the types and phylogenetic associations were analyzed using FastTree 2.1.5 (data not shown) (85).

We analyzed the phylogenetic position of *narG* encoded in our genomes by putting these genes in the context of known denitrifying taxa, other *Methylococcales*, other methanotrophs, and genes of distant taxa retrieved from NCBI that were similar to the divergent *narG* gene identified in some *Methylococcales* species. The phylogeny was generated using the substitution model determined by ProTest. We computationally examined the substrate and cofactor binding residues (45) of inferred peptide sequences to provide additional support for the possible activity of these genes. The putative structures of OWC *Methylobacter* and NSP1-2 *narG* were submitted to SWISS-MODEL (https://swissmodel.expasy.org/) (95) for comparison to model NarG encoded by *E. coli* (PDB code 1q16.1.A).

Identification of *Methylococcaceae* OWC *pmoA* sequences in public data sets. Soil (subset of the terrestrial set) and freshwater (subset of the aquatic set) habitat metagenomes and metatranscriptomes publicly available on IMG/M were searched (February 2017) for genes similar to OWC *Methylobacter* and NSP1-2 *pmoA* genes using the BLASTp function with an E value cutoff of 1e−20. We also mined previous publications emphasizing the importance of *M. tundripaludum*-like *pmoA* sequences in environmental methane cycling and environmental sequences similar to OWC *Methylobacter* or NSP1-2 genes available on NCBI. These included data from Tveit et al. (14), Liebner et al. (29), Martineau et al. (62), and Samad and Bertilsson (96), which are available as Short Read Archives on NCBI under the following accession numbers: SRA SRR524822 and SRR524823, PopSet 159135051, PopSet 300679917, and PopSet 498541747, respectively. Hits that were fewer than 130 amino acids or 400 nucleotides in length (~50% the total length) were removed from further analyses.

The combination of these filtered databases totaled 2,941 genes and 2,889 peptides from environmental sequence databases. These sequences were aligned to full-length OWC *Methylobacter* sequences (NSM2-1 and NSP1-1), NSP1-2, and reference *Methylococcales* sequences using MUSCLE 3.8.31. A maximum likelihood phylogenetic tree of the reference sequences was generated using RAxML 8.3.1 with 100 bootstraps for both nucleotide and amino acid alignments and GTRGAMMA and GAMMAWAG (11), respectively. Environmental sequences were computationally assigned to nodes using *pplacer* (97), and the specific position of the placement was determined by identifying the node with the greatest log likelihood. Hits that were placed specifically onto NSM2-1, NSP1-1, or NSP1-2 in at least the nucleotide or amino acid analysis were considered to be affiliated with the OWC *Methylobacter* or NSP1-2 and not with neighboring members. To generate Fig. S7, only the hits following these criteria were reanalyzed with *pplacer* using the same reference tree, and the resuts were appended to their branch placements with *guppy* (97). The initial assignments of the hits obtained using *pplacer* are available in Data Set S1.

Statistical analyses and visualization. Statistical analyses and data visualizations, including phylogenies, were performed in R 3.3.2, while the methanol dehydrogenase tree was visualized using the interactive Tree Of Life method (iTOL [http://itol.embl.de/]) (98). Significant differences were detected by analysis of variance with *post hoc* correction for multiple comparisons using Tukey's honest significant difference tests and were defined as an adjusted *P* value of less than 0.05 computed using the "stats" package (*aov* with *TukeyHSD*). Correlations were significant (and are reported here) only in cases in which the *R* value was less than −0.5 or exceeded +0.5, and a *P* value of less than 0.05 as calculated by the use of the "Hmisc" package (*rcorr*). Relationships among relative abundance, gene expression, and geochemical gradient variables were calculated and visualized by fitting to a simple linear model using quantile regression as part of the "stats" package (*lm*). The positions of environmental sequences assigned to our genomes were extracted using the "ggtree" package (*get.placements*).

Metagenomic and metatranscriptomic pipelines. The commands used for metagenomic and metatranscriptomic computations can be accessed via respective repositories on our GitHub page (https://github.com/TheWrightonLab/).

Accession number(s). Methanotroph genomes generated here are available on NCBI under the following accession numbers (Data Set S1): SAMN05908750 (NSM2-1), SAMN05908751 (NSO1-1), SAMN05908747 (NSP1-1), SAMN05908748 (NSP1-2). Metagenomes and metatranscriptomes can be accessed via NCBI under the following BioSample numbers: SAMN06267298 (November 2014 plant metagenome), SAMN05892948 (November 2014 water metagenome), SAMN05892929 (November 2014 plant metagenome), SAMN06267290 (August 2015 mud metagenome), SAMN06267291 (August 2015 water metagenome), and SAMN06267292 (August 2015 plant metagenome), and SAMN06267298, SAMN06267299, SAMN06267300, SAMN06267301, SAMN06267302, SAMN06267303, SAMN06267304, SAMN06267305, SAMN06267306, SAMN06267307, SAMN06267308, and SAMN06267309 (November 2014 and August 2015 metatranscriptomes). 16S rRNA gene amplicon sequencing data can be retrieved from NCBI under BioProject PRJNA338276.

SUPPLEMENTAL MATERIAL

Supplemental material for this article may be found at https://doi.org/10.1128/mBio.00815-18.

TEXT S1, DOCX file, 0.1 MB.
FIG S1, EPS file, 0.9 MB.
FIG S2, EPS file, 1.3 MB.
FIG S3, EPS file, 1.3 MB.
FIG S4, EPS file, 1.3 MB.
FIG S5, PDF file, 0.4 MB.
FIG S6, EPS file, 1 MB.
FIG S7, EPS file, 1.3 MB.
DATASET S1, XLSX file, 2 MB.
DATASET S2, XLSX file, 2.4 MB.

ACKNOWLEDGMENTS

We thank Ludmila Chistoserdova at the University of Washington, as well as anonymous reviewers, as their feedback greatly improved the manuscript. We thank Kristi Arend, Frank Lopez, and the rest of the OWC staff for site access and logistical support. We also grateful to Austin Rechner, Dominique Haddad, Sharon Acosta, and Chante Vines for their assistance with field work and measurements. We thank the staff members at the Ohio Supercomputer Center for allocating time and resources for data processing.

This effort was supported by an Early Career Award from the U.S. Department of Energy (DOE), Office of Science, Office of Biological and Environmental Research, under award number DE-SC0018022 to K.C.W. This material is based upon work supported by the National Science Foundation Graduate Research Fellowship under grant no. DGE-1343012 to G.J.S. T.H.M. was partially supported by a Doctoral Dissertation Improvement Grant from NSF and by a Department of Energy (DOE) Office of Science Graduate Research Program, Solicitation 2. DNA and RNA sequencing awarded to K.C.W. was conducted by the U.S. Department of Energy Joint Genome Institute, a DOE Office of Science User Facility that is supported by the Office of Science of the U.S. Department of Energy under contract no. DE-AC02-05CH11231. Flux observations were conducted by G.B. with support from the Office of Science of the U.S. Department of Energy, Ameriflux Management project.

REFERENCES

1. Bridgham SD, Cadillo-Quiroz H, Keller JK, Zhuang Q. 2013. Methane emissions from wetlands: biogeochemical, microbial, and modeling perspectives from local to global scales. Glob Change Biol 19:1325–1346. https://doi.org/10.1111/gcb.12131.
2. Kirschke S, Bousquet P, Ciais P, Saunois M, Canadell JG, Dlugokencky EJ, Bergamaschi P, Bergmann D, Blake DR, Bruhwiler L, Cameron-Smith P, Castaldi S, Chevallier F, Feng L, Fraser A, Heimann M, Hodson EL, Houweling S, Josse B, Fraser PJ, Krummel PB, Lamarque J-F, Langenfelds RL, Le Quéré C, Naik V, O'Doherty S, Palmer PI, Pison I, Plummer D, Poulter B, Prinn RG, Rigby M, Ringeval B, Santini M, Schmidt M, Shindell DT, Simpson IJ, Spahni R, Steele LP, Strode SA, Sudo K, Szopa S, van der Werf GR, Voulgarakis A, van Weele M, Weiss RF, Williams JE, Zeng G. 2013. Three decades of global methane sources and sinks. Nature Geosci 6:813–823. https://doi.org/10.1038/ngeo1955.
3. Laanbroek HJ. 2010. Methane emission from natural wetlands: interplay between emergent macrophytes and soil microbial processes. A minireview. Ann Bot 105:141–153. https://doi.org/10.1093/aob/mcp201.
4. Paudel R, Mahowald NM, Hess PG, Meng L, Riley WJ. 2016. Attribution of changes in global wetland methane emissions from pre-industrial to present using CLM4.5-BGC. Environ Res Lett 11:034020. https://doi.org/10.1088/1748-9326/11/3/034020.
5. Bethke CM, Sanford RA, Kirk MF, Jin Q, Flynn TM. 2011. The thermodynamic ladder in geomicrobiology. Am J Sci 311:183–210. https://doi.org/10.2475/03.2011.01.
6. Riley WJ, Subin ZM, Lawrence DM, Swenson SC, Torn MS, Meng L, Mahowald NM, Hess P. 2011. Barriers to predicting changes in global terrestrial methane fluxes: analyses using CLM4Me, a methane biogeochemistry model integrated in CESM. Biogeosciences 8:1925–1953. https://doi.org/10.5194/bg-8-1925-2011.
7. Dumont MG, Pommerenke B, Casper P. 2013. Using stable isotope probing to obtain a targeted metatranscriptome of aerobic methanotrophs in lake sediment. Environ Microbiol Rep 5:757–764. https://doi.org/10.1111/1758-2229.12078.
8. Kits KD, Campbell DJ, Rosana AR, Stein LY. 2015. Diverse electron sources support denitrification under hypoxia in the obligate methanotroph Methylomicrobium album strain BG8. Front Microbiol 6:1072. https://doi.org/10.3389/fmicb.2015.01072.
9. Kits KD, Klotz MG, Stein LY. 2015. Methane oxidation coupled to nitrate reduction under hypoxia by the Gammaproteobacterium Methylomonas denitrificans, sp. nov. type strain FJG1. Environ Microbiol 17:3219–3232. https://doi.org/10.1111/1462-2920.12772.
10. Padilla CC, Bertagnolli AD, Bristow LA, Sarode N, Glass JB, Thamdrup B, Stewart FJ. 2017. Metagenomic binning recovers a transcriptionally active Gammaproteobacterium linking methanotrophy to partial denitrification in an anoxic oxygen minimum zone. Front Mar Sci 4. https://doi.org/10.3389/fmars.2017.00023.
11. Oswald K, Graf JS, Littmann S, Tienken D, Brand A, Wehrli B, Albertsen M, Daims H, Wagner M, Kuypers MM. 2017. Crenothrix are major methane consumers in stratified lakes. ISME J 11:2124–2140. https://doi.org/10.1038/ismej.2017.77.
12. Skennerton CT, Ward LM, Michel A, Metcalfe K, Valiente C, Mullin S, Chan KY, Gradinaru V, Orphan VJ. 2015. Genomic reconstruction of an uncultured hydrothermal vent gammaproteobacterial methanotroph (family Methylothermaceae) indicates multiple adaptations to oxygen limitation. Front Microbiol 6:1425. https://doi.org/10.3389/fmicb.2015.01425.
13. Stein LY, Klotz MG. 2011. Nitrifying and denitrifying pathways of methanotrophic bacteria. Biochem Soc Trans. 39:1826–1831. https://doi.org/10.1042/BST20110712.
14. Tveit A, Schwacke R, Svenning MM, Urich T. 2013. Organic carbon transformations in high-Arctic peat soils: key functions and microorganisms. ISME J 7:299–311. https://doi.org/10.1038/ismej.2012.99.
15. Angel R, Matthies D, Conrad R. 2011. Activation of methanogenesis in arid biological soil crusts despite the presence of oxygen. PLoS One 6:e20453. https://doi.org/10.1371/journal.pone.0020453.
16. Angle JC, Morin TH, Solden LM, Narrowe AB, Smith GJ, Borton MA, Rey-Sanchez C, Daly RA, Mirfenderesgi G, Hoyt DW, Riley WJ, Miller CS, Bohrer G, Wrighton KC. 2017. Methanogenesis in oxygenated soils is a substantial fraction of wetland methane emissions. Nat Commun 8:1567. https://doi.org/10.1038/s41467-017-01753-4.
17. Teh YA, Silver WL, Conrad ME. 2005. Oxygen effects on methane production and oxidation in humid tropical forest soils. Global Change Biol 11:1283–1297. https://doi.org/10.1111/j.1365-2486.2005.00983.x.
18. Rey-Sanchez AC, Morin TH, Stefanik KC, Wrighton K, Bohrer G. 2018. Determining total emissions and environmental drivers of methane flux in a Lake Erie estuarine marsh. Ecological Engineering 114:7–15. https://doi.org/10.1016/j.ecoleng.2017.06.042.
19. Narrowe AB, Angle JC, Daly RA, Stefanik KC, Wrighton KC, Miller CS. 2017. High-resolution sequencing reveals unexplored archaeal diversity in freshwater wetland soils. Environ Microbiol 19:2192–2209. https://doi.org/10.1111/1462-2920.13703.
20. Chistoserdova L. 2011. Methylotrophy in a lake: from metagenomics to single-organism physiology. Appl Environ Microbiol 77:4705–4711. https://doi.org/10.1128/AEM.00314-11.
21. Wartiainen I, Hestnes AG, McDonald IR, Svenning MM. 2006. Methylobacter tundripaludum sp. nov., a methane-oxidizing bacterium from Arctic wetland soil on the Svalbard islands, Norway (78 degrees N). Int J Syst Evol Microbiol 56:109–113. https://doi.org/10.1099/ijs.0.63728-0.
22. Hamilton R, Kits KD, Ramonovskaya VA, Rozova ON, Yurimoto H, Iguchi H, Khmelenina VN, Sakai Y, Dunfield PF, Klotz MG. 2015. Draft genomes of gammaproteobacterial methanotrophs isolated from terrestrial ecosystems. Genome Announc 3:e00515-15. https://doi.org/10.1128/genomeA.00515-15.
23. Flynn JD, Hirayama H, Sakai Y, Dunfield PF, Klotz MG, Knief C, Op den Camp HJM, Jetten MS, Khmelenina VN, Trotsenko YA., Murrell JC, Semrau JD, Svenning MM, Stein LY, Kyrpides N, Shapiro N, Woyke T, Bringel F, Vuilleumier S, DiSpirito AA, Kalyuzhnaya MG. 2016. Draft genome sequences of gammaproteobacterial methanotrophs isolated from marine ecosystems. Genome Announc 4:e01629-15. https://doi.org/10.1128/genomeA.01629-15.
24. Mysara M, Vandamme P, Props R, Kerckhof F-M, Leys N, Boon N, Raes J, Monsieurs P. 2017. Reconciliation between operational taxonomic units and species boundaries. FEMS Microbiol Ecol 93:fix029. https://doi.org/10.1093/femsec/fix029.
25. Bowers RM, Kyrpides NC, Stepanauskas R, Harmon-Smith M, Doud D, Reddy TBK, Schulz F, Jarett J, Rivers AR, Eloe-Fadrosh EA, Tringe SG, Ivanova NN, Copeland A, Clum A, Becraft ED, Malmstrom RR, Birren B, Podar M, Bork P, Weinstock GM, Garrity GM, Dodsworth JA, Yooseph S, Sutton G, Glöckner FO, Gilbert JA, Nelson WC, Hallam SJ, Jungbluth SP, Ettema TJG, Tighe S, Konstantinidis KT, Liu W-T, Baker BJ, Rattei T, Eisen JA, Hedlund B, McMahon KD, Fierer N, Knight R, Finn R, Cochrane G, Karsch-Mizrachi I, Tyson GW, Rinke C, Kyrpides NC, Schriml L, Garrity GM, Hugenholtz P, Sutton G, et al. 2017. Minimum information about a single amplified genome (MISAG) and a metagenome-assembled genome (MIMAG) of bacteria and archaea. Nat Biotechnol 35:725. https://doi.org/10.1038/nbt.3893.
26. Miller CS, Baker BJ, Thomas BC, Singer SW, Banfield JF. 2011. EMIRGE: reconstruction of full-length ribosomal genes from microbial community short read sequencing data. Genome Biol 12:R44. https://doi.org/10.1186/gb-2011-12-5-r44.
27. McDonald IR, Bodrossy L, Chen Y, Murrell JC. 2008. Molecular ecology techniques for the study of aerobic methanotrophs. Appl Environ Microbiol 74:1305–1315. https://doi.org/10.1128/AEM.02233-07.
28. Knief C. 2015. Diversity and habitat preferences of cultivated and uncultivated aerobic methanotrophic bacteria evaluated based on pmoA as molecular marker. Front Microbiol 6:1346. https://doi.org/10.3389/fmicb.2015.01346.
29. Liebner S, Rublack K, Stuehrmann T, Wagner D. 2009. Diversity of aerobic methanotrophic bacteria in a permafrost active layer soil of the Lena Delta, Siberia. Microb Ecol 57:25–35. https://doi.org/10.1007/s00248-008-9411-x.
30. Parks DH, Chuvochina M, Waite DW, Rinke C, Skarshewski A, Chaumeil PA, Hugenholtz P. 2018. A standardized bacterial taxonomy based on genome phylogeny substantially revises the tree of life. Nat Biotechnol 36:996–1004. https://doi.org/10.1038/nbt.4229.
31. Edwards CR, Onstott TC, Miller JM, Wiggins JB, Wang W, Lee CK, Cary SC, Pointing SB, Lau MCY. 2017. Draft genome sequence of uncultured upland soil cluster Gammaproteobacteria gives molecular insights into high-affinity methanotrophy. Genome Announc 5:e00047-17. https://doi.org/10.1128/genomeA.00047-17.
32. Keltjens JT, Pol A, Reimann J, Op den Camp HJ. 2014. PQQ-dependent methanol dehydrogenases: rare-earth elements make a difference. Appl

Microbiol Biotechnol 98:6163–6183. https://doi.org/10.1007/s00253-014-5766-8.
33. Pol A, Barends TRM, Dietl A, Khadem AF, Eygensteyn J, Jetten MSM, Op den Camp HJM. 2014. Rare earth metals are essential for methanotrophic life in volcanic mudpots. Environ Microbiol 16:255–264. https://doi.org/10.1111/1462-2920.12249.
34. Ramachandran A, Walsh DA. 2015. Investigation of XoxF methanol dehydrogenases reveals new methylotrophic bacteria in pelagic marine and freshwater ecosystems. FEMS Microbiol Ecol 91:fiv105. https://doi.org/10.1093/femsec/fiv105.
35. Giovannoni SJ, Hayakawa DH, Tripp HJ, Stingl U, Givan SA, Cho JC, Oh HM, Kitner JB, Vergin KL, Rappé MS. 2008. The small genome of an abundant coastal ocean methylotroph. Environ Microbiol 10:1771–1782. https://doi.org/10.1111/j.1462-2920.2008.01598.x.
36. Mustakhimov I, Kalyuzhnaya MG, Lidstrom ME, Chistoserdova L. 2013. Insights into denitrification in Methylotenera mobilis from denitrification pathway and methanol metabolism mutants. J Bacteriol 195:2207–2211. https://doi.org/10.1128/JB.00069-13.
37. Jewell T, Huston SL, Nelson DC. 2008. Methylotrophy in freshwater Beggiatoa alba strains. Appl Environ Microbiol 74:5575–5578. https://doi.org/10.1128/AEM.00379-08.
38. Beck DA, McTaggart TL, Setboonsarng U, Vorobev A, Kalyuzhnaya MG, Ivanova N, Goodwin L, Woyke T, Lidstrom ME, Chistoserdova L. 2014. The expanded diversity of methylophilaceae from Lake Washington through cultivation and genomic sequencing of novel ecotypes. PLoS One 9:e102458. https://doi.org/10.1371/journal.pone.0102458.
39. Borisov VB, Gennis RB, Hemp J, Verkhovsky MI. 2011. The cytochrome bd respiratory oxygen reductases. Biochim Biophys Acta 1807:1398–1413. https://doi.org/10.1016/j.bbabio.2011.06.016.
40. Tavormina PL, Orphan VJ, Kalyuzhnaya MG, Jetten MSM, Klotz MG. 2011. A novel family of functional operons encoding methane/ammonia monooxygenase-related proteins in gammaproteobacterial methanotrophs. Environ Microbiol Rep 3:91–100. https://doi.org/10.1111/j.1758-2229.2010.00192.x.
41. Krause SM, Johnson T, Karunaratne YS, Fu Y, Beck DA, Chistoserdova L, Lidstrom ME. 2017. Lanthanide-dependent cross-feeding of methane-derived carbon is linked by microbial community interactions. Proc Natl Acad Sci U S A 114:358–363. https://doi.org/10.1073/pnas.1619871114.
42. Muras V, Dogaru-Kinn P, Minato Y, Häse CC, Steuber J. 2016. The Na+-translocating NADH:quinone oxidoreductase enhances oxidative stress in the cytoplasm of Vibrio cholerae. J Bacteriol 198:2307–2317. https://doi.org/10.1128/JB.00342-16.
43. Chistoserdova L. 2015. Methylotrophs in natural habitats: current insights through metagenomics. Appl Microbiol Biotechnol 99:5763–5779. https://doi.org/10.1007/s00253-015-6713-z.
44. Chistoserdova L, Kalyuzhnaya MG, Lidstrom ME. 2009. The expanding world of methylotrophic metabolism. Annu Rev Microbiol 63:477–499. https://doi.org/10.1146/annurev.micro.091208.073600.
45. Castelle CJ, Hug LA, Wrighton KC, Thomas BC, Williams KH, Wu D, Tringe SG, Singer SW, Eisen JA, Banfield JF. 2013. Extraordinary phylogenetic diversity and metabolic versatility in aquifer sediment. Nat Commun 4. https://doi.org/10.1038/ncomms3120.
46. Anderson B, Bartlett KB, Frolking S, Hayhoe K, Jenkins JC, Salas WA. 2010. Methane and nitrous oxide emissions from natural sources. Office of Atmospheric Programs, U.S. EPA, Washington, DC.
47. Kalyuzhnaya MG, Yang S, Rozova ON, Smalley NE, Clubb J, Lamb A, Gowda GA, Raftery D, Fu Y, Bringel F, Vuilleumier S, Beck DA, Trotsenko YA, Khmelenina VN, Lidstrom ME. 2013. Highly efficient methane biocatalysis revealed in a methanotrophic bacterium. Nat Commun 4:2785. https://doi.org/10.1038/ncomms3785.
48. Gilman A, Fu Y, Hendershott M, Chu F, Puri AW, Smith AL, Pesesky M, Lieberman R, Beck DA, Lidstrom ME. 2017. Oxygen-limited metabolism in the methanotroph Methylomicrobium buryatense 5GB1C. PeerJ 5:e3945. https://doi.org/10.7717/peerj.3945.
49. Carere CR, Hards K, Houghton KM, Power JF, McDonald B, Collet C, Gapes DJ, Sparling R, Boyd ES, Cook GM, Greening C, Stott MB. 2017. Mixotrophy drives niche expansion of verrucomicrobial methanotrophs. ISME J 11:2599. https://doi.org/10.1038/ismej.2017.112.
50. Mohammadi S, Pol A, van Alen TA, Jetten MS, den Camp HJO. 2017. Methylacidiphilum fumariolicum SolV, a thermoacidophilic 'Knallgas' methanotroph with both an oxygen-sensitive and-insensitive hydrogenase. ISME J 11:945. https://doi.org/10.1038/ismej.2016.171.
51. Bailly X, Vanin S, Chabasse C, Mizuguchi K, Vinogradov SN. 2008. A phylogenomic profile of hemerythrins, the nonheme diiron binding respiratory proteins. BMC Evol Biol 8:244. https://doi.org/10.1186/1471-2148-8-244.
52. Chen KH-C, Wu H-H, Ke S-F, Rao Y-T, Tu C-M, Chen Y-P, Kuei K-H, Chen Y-S, Wang VC-C, Kao W-C, Chan SI. 2012. Bacteriohemerythrin bolsters the activity of the particulate methane monooxygenase (pMMO) in Methylococcus capsulatus (Bath). J Inorg Biochem 111:10–17. https://doi.org/10.1016/j.jinorgbio.2012.02.019.
53. Kao W-C, Chen Y-R, Yi EC, Lee H, Tian Q, Wu K-M, Tsai S-F, Yu SS-F, Chen Y-J, Aebersold R, Chan SI. 2004. Quantitative proteomic analysis of metabolic regulation by copper ions in Methylococcus capsulatus (Bath). J Biol Chem 279:51554–51560. https://doi.org/10.1074/jbc.M408013200.
54. Kao W-C, Wang VC-C, Huang Y-C, Yu SS-F, Chang T-C, Chan SI. 2008. Isolation, purification and characterization of hemerythrin from Methylococcus capsulatus (Bath). J Inorg Biochem 102:1607–1614. https://doi.org/10.1016/j.jinorgbio.2008.02.008.
55. Karlsen OA, Ramsevik L, Bruseth LJ, Larsen Ø, Brenner A, Berven FS, Jensen HB, Lillehaug JR. 2005. Characterization of a prokaryotic haemerythrin from the methanotrophic bacterium Methylococcus capsulatus (Bath). FEBS J 272:2428–2440. https://doi.org/10.1111/j.1742-4658.2005.04663.x.
56. Schaller RA, Ali SK, Klose KE, Kurtz JDM. 2012. A bacterial hemerythrin domain regulates the activity of a Vibrio cholerae diguanylate cyclase. Biochemistry 51:8563–8570. https://doi.org/10.1021/bi3011797.
57. Belova S, Oshkin IY, Glagolev M, Lapshina E, Maksyutov SS, Dedysh S. 2013. Methanotrophic bacteria in cold seeps of the floodplains of northern rivers. Microbiology 82:743–750. https://doi.org/10.1134/S0026261713060040.
58. Berestovskaya YY, Vasil'eva L, Chestnykh O, Zavarzin G. 2002. Methanotrophs of the psychrophilic microbial community of the Russian Arctic tundra. Mikrobiologiia 71:538–544. (In Russian.)
59. Graef C, Hestnes AG, Svenning MM, Frenzel P. 2011. The active methanotrophic community in a wetland from the High Arctic. Environ Microbiol Rep 3:466–472. https://doi.org/10.1111/j.1758-2229.2010.00237.x.
60. Kallistova AY, Montonen L, Jurgens G, Münster U, Kevbrina MV, Nozhevnikova AN. 2013. Culturable psychrotolerant methanotrophic bacteria in landfill cover soil. Microbiology 82:847–855. https://doi.org/10.1134/S0026261714010044.
61. Michaud AB, Dore JE, Achberger AM, Christner BC, Mitchell AC, Skidmore ML, Vick-Majors TJ, Priscu JC. 2017. Microbial oxidation as a methane sink beneath the West Antarctic Ice Sheet. Nature Geosci 10:582. https://doi.org/10.1038/ngeo2992.
62. Martineau C, Whyte LG, Greer CW. 2010. Stable isotope probing analysis of the diversity and activity of methanotrophic bacteria in soils from the Canadian High Arctic. Appl Environ Microbiol 76:5773–5784. https://doi.org/10.1128/AEM.03094-09.
63. Omel'Chenko M, Vasil'Eva L, Zavarzin G, Savel'Eva N, Lysenko A, Mityushina L, Khmelenina V, Trotsenko YA. 1996. A novel psychrophilic methanotroph of the genus Methylobacter. Microbiology 65:339–343.
64. Ren T, Roy R, Knowles R. 2000. Production and consumption of nitric oxide by three methanotrophic bacteria. Appl Environ Microbiol 66:3891–3897. https://doi.org/10.1128/AEM.66.9.3891-3897.2000.
65. Svenning MM, Hestnes AG, Wartiainen I, Stein LY, Klotz MG, Kalyuzhnaya MG, Spang A, Bringel F, Vuilleumier S, Lajus A, Médigue C, Bruce DC, Cheng JF, Goodwin L, Ivanova N, Han J, Han CS, Hauser L, Held B, Land ML, Lapidus A, Lucas S, Nolan M, Pitluck S, Woyke T. 2011. Genome sequence of the Arctic methanotroph Methylobacter tundripaludum SV96. J Bacteriol 193:6418–6419. https://doi.org/10.1128/JB.05380-11.
66. Tveit AT, Urich T, Frenzel P, Svenning MM. 2015. Metabolic and trophic interactions modulate methane production by Arctic peat microbiota in response to warming. Proc Natl Acad Sci U S A 112:E2507–E2516. https://doi.org/10.1073/pnas.1420797112.
67. Tveit A, Urich T, Svenning MM. 2014. Metatranscriptomic analysis of Arctic peat soil microbiota. Appl Environ Microbiol 80:5761–5772. https://doi.org/10.1128/AEM.01030-14.
68. Mondav R, Woodcroft BJ, Kim E-H, McCalley CK, Hodgkins SB, Crill PM, Chanton J, Hurst GB, VerBerkmoes NC, Saleska SR, Hugenholtz P, Rich VI, Tyson GW. 2014. Discovery of a novel methanogen prevalent in thawing permafrost. Nat Commun 5:3212. https://doi.org/10.1038/ncomms4212.
69. Kalyuzhnaya MG, Lamb AE, McTaggart TL, Oshkin IY, Shapiro N, Woyke T, Chistoserdova L. 2015. Draft genome sequences of gammaproteobacterial methanotrophs isolated from Lake Washington sediment. Genome Announc 3:e00103-15. https://doi.org/10.1128/genomeA.00103-15.
70. Dalcin Martins P, Hoyt DW, Bansal S, Mills CT, Tfaily M, Tangen BA, Finocchiaro RG, Johnston MD, McAdams BC, Solensky MJ. 2017. Abun-

dant carbon substrates drive extremely high sulfate reduction rates and methane fluxes in prairie pothole wetlands. Glob Chang Biol 23:3107–3120. https://doi.org/10.1111/gcb.13633.
71. He S, Malfatti SA, McFarland JW, Anderson FE, Pati A, Huntemann M, Tremblay J, Glavina del Rio T, Waldrop MP, Windham-Myers L, Tringe SG. 2015. Patterns in wetland microbial community composition and functional gene repertoire associated with methane emissions. mBio 6:e00066-15. https://doi.org/10.1128/mBio.00066-15.
72. King GM, Roslev P, Skovgaard H. 1990. Distribution and rate of methane oxidation in sediments of the Florida Everglades. Appl Environ Microbiol 56:2902–2911.
73. Lawrence BA, Lishawa SC, Hurst N, Castillo BT, Tuchman NC. 2017. Wetland invasion by Typha× glauca increases soil methane emissions. Aquat Bot 137:80–87. https://doi.org/10.1016/j.aquabot.2016.11.012.
74. Morin TH, Bohrer G, Frasson RPDM, Naor-Azreli L, Mesi S, Stefanik KC, Schäfer KVR. 2014. Environmental drivers of methane fluxes from an urban temperate wetland park. J Geophys Res Biogeosci 119:2188–2208. https://doi.org/10.1002/2014JG002750.
75. Chan A, Parkin T. 2001. Methane oxidation and production activity in soils from natural and agricultural ecosystems. J Environ Qual 30:1896–1903. https://doi.org/10.2134/jeq2001.1896.
76. Caporaso JG, Lauber CL, Walters WA, Berg-Lyons D, Huntley J, Fierer N, Owens SM, Betley J, Fraser L, Bauer M, Gormley N, Gilbert JA, Smith G, Knight R. 2012. Ultra-high-throughput microbial community analysis on the Illumina HiSeq and MiSeq platforms. ISME J 6:1621–1624. https://doi.org/10.1038/ismej.2012.8.
77. Solden LM, Hoyt DW, Collins WB, Plank JE, Daly RA, Hildebrand E, Beavers TJ, Wolfe R, Nicora CD, Purvine SO, Carstensen M, Lipton MS, Spalinger DE, Firkins JL, Wolfe BA, Wrighton KC. 2017. New roles in hemicellulosic sugar fermentation for the uncultivated Bacteroidetes family BS11. ISME J 11:691–703. https://doi.org/10.1038/ismej.2016.150.
78. Peng Y, Leung HC, Yiu SM, Chin FY. 2012. IDBA-UD: a de novo assembler for single-cell and metagenomic sequencing data with highly uneven depth. Bioinformatics 28:1420–1428. https://doi.org/10.1093/bioinformatics/bts174.
79. Wrighton KC, Thomas BC, Sharon I, Miller CS, Castelle CJ, VerBerkmoes NC, Wilkins MJ, Hettich RL, Lipton MS, Williams KH, Long PE, Banfield JF. 2012. Fermentation, hydrogen, and sulfur metabolism in multiple uncultivated bacterial phyla. Science 337:1661–1665. https://doi.org/10.1126/science.1224041.
80. Dick GJ, Andersson AF, Baker BJ, Simmons SL, Thomas BC, Yelton AP, Banfield JF. 2009. Community-wide analysis of microbial genome sequence signatures. Genome Biol 10:R85. https://doi.org/10.1186/gb-2009-10-8-r85.
81. Wu M, Scott AJ. 2012. Phylogenomic analysis of bacterial and archaeal sequences with AMPHORA2. Bioinformatics 28:1033–1034. https://doi.org/10.1093/bioinformatics/bts079.
82. Langmead B, Salzberg SL. 2012. Fast gapped-read alignment with Bowtie 2. Nat Methods 9:357–359. https://doi.org/10.1038/nmeth.1923.
83. Trapnell C, Williams BA, Pertea G, Mortazavi A, Kwan G, Van Baren MJ, Salzberg SL, Wold BJ, Pachter L. 2010. Transcript assembly and quantification by RNA-Seq reveals unannotated transcripts and isoform switching during cell differentiation. Nat Biotechnol 28:511–515. https://doi.org/10.1038/nbt.1621.
84. Markowitz VM, Chen I-MA, Palaniappan K, Chu K, Szeto E, Grechkin Y, Ratner A, Jacob B, Huang J, Williams P, Huntemann M, Anderson I, Mavromatis K, Ivanova NN, Kyrpides NC. 2012. IMG: the integrated microbial genomes database and comparative analysis system. Nucleic Acids Res 40:D115–D122. https://doi.org/10.1093/nar/gkr1044.
85. Price MN, Dehal PS, Arkin AP. 2010. FastTree 2–approximately maximum-likelihood trees for large alignments. PLoS One 5:e9490. https://doi.org/10.1371/journal.pone.0009490.
86. Edgar RC. 2004. MUSCLE: multiple sequence alignment with high accuracy and high throughput. Nucleic Acids Res 32:1792–1797. https://doi.org/10.1093/nar/gkh340.
87. Olsen C, Qaadri K, Moir R, Kearse M, Buxton S, Cheung M. Geneious R7: a bioinformatics platform for biologists. Biomatters, Inc., Newark, NJ.
88. Stamatakis A. 2014. RAxML version 8: a tool for phylogenetic analysis and post-analysis of large phylogenies. Bioinformatics 30:1312–1313. https://doi.org/10.1093/bioinformatics/btu033.
89. Yilmaz P, Parfrey LW, Yarza P, Gerken J, Pruesse E, Quast C, Schweer T, Peplies J, Ludwig W, Glöckner FO. 2014. The SILVA and "all-species living tree project (LTP)" taxonomic frameworks. Nucleic Acids Res 42:D643–D648. https://doi.org/10.1093/nar/gkt1209.
90. Rinke C, Schwientek P, Sczyrba A, Ivanova NN, Anderson IJ, Cheng J-F, Darling A, Malfatti S, Swan BK, Gies EA, Dodsworth JA, Hedlund BP, Tsiamis G, Sievert SM, Liu W-T, Eisen JA, Hallam SJ, Kyrpides NC, Stepanauskas R, Rubin EM, Hugenholtz P, Woyke T. 2013. Insights into the phylogeny and coding potential of microbial dark matter. Nature 499:431–437. https://doi.org/10.1038/nature12352.
91. Hug LA, Baker BJ, Anantharaman K, Brown CT, Probst AJ, Castelle CJ, Butterfield CN, Hernsdorf AW, Amano Y, Ise K, Suzuki Y, Dudek N, Relman DA, Finstad KM, Amundson R, Thomas BC, Banfield JF. 2016. A new view of the tree of life. Nat Microbiol 1:16048. https://doi.org/10.1038/nmicrobiol.2016.48.
92. Taubert M, Grob C, Howat AM, Burns OJ, Dixon JL, Chen Y, Murrell JC. 2015. XoxF encoding an alternative methanol dehydrogenase is widespread in coastal marine environments. Environ Microbiol 17:3937–3948. https://doi.org/10.1111/1462-2920.12896.
93. Chu F, Lidstrom ME. 2016. XoxF acts as the predominant methanol dehydrogenase in the type I methanotroph Methylomicrobium buryatense. J Bacteriol 198:1317–1325. https://doi.org/10.1128/JB.00959-15.
94. Abascal F, Zardoya R, Posada D. 2005. ProtTest: selection of best-fit models of protein evolution. Bioinformatics 21:2104–2105. https://doi.org/10.1093/bioinformatics/bti263.
95. Biasini M, Bienert S, Waterhouse A, Arnold K, Studer G, Schmidt T, Kiefer F, Gallo Cassarino T, Bertoni M, Bordoli L, Schwede T. 2014. SWISS-MODEL: modelling protein tertiary and quaternary structure using evolutionary information. Nucleic Acids Res 42:W252–W258. https://doi.org/10.1093/nar/gku340.
96. Samad MS, Bertilsson S. 2017. Seasonal variation in abundance and diversity of bacterial methanotrophs in five temperate lakes. Front Microbiol 8:142. https://doi.org/10.3389/fmicb.2017.00142.
97. Matsen FA, Kodner RB, Armbrust EV. 2010. pplacer: linear time maximum-likelihood and Bayesian phylogenetic placement of sequences onto a fixed reference tree. BMC Bioinformatics 11:538. https://doi.org/10.1186/1471-2105-11-538.
98. Letunic I, Bork P. 2016. Interactive tree of life (iTOL) v3: an online tool for the display and annotation of phylogenetic and other trees. Nucleic Acids Res 44:W242–W245. https://doi.org/10.1093/nar/gkw290.